ORIGINAL ARTICLES

CANCER CELL SURVIVAL MODEL AFTER PHOTODYNAMIC THERAPY

Karami-Gadallo L., Pouladian M.
Islamic Azad University, Tehran, Iran

Abstract

Photodynamic therapy (PDT) is known as a routine treatment method in which cell survival index like viability plotted versus $^1O_2$ concentration or light fluence in the form of a curve. In this paper, a mathematical model was proposed with ability of generating a mirrored-sigmoid curve which seems to be fitted to any experimental data relating to cell viability, survival probability or any cellular index representing living conditions through adjusting three parameters. It was validated by showing an excellent curve fitting relatively with data obtained from cancerous lung cells under ALA-PDT process in vitro.

It was tried to define the relations between model's parameters and biological/clinical factors with the curve regions of plateau (at low doses; non-sensitive part), steep (high-sensitive part), and steady state (at high doses; low-sensitive part). It seems this model could be excellently fitted to any data presenting the cell-living index versus the killer agent in «any cancer therapy technique (e.g. radiotherapy)». Although this claim showed to be correct for PDT, different relevant data of other researchers should also be used for this model and other usual models too, in order to compare their fitness rates.

Key words: cell survival curve, mathematical modeling, photodynamic therapy.

For citations: Karami-Gadallo L., Pouladian M. Cancer cell survival model after photodynamic therapy, *Biomedical Photonics*, 2022, vol. 11, no. 2, pp. 4–11. doi: 10.24931/2413–9432–2022–11-2–4–11.

Contacts: L. Karami-Gadallo, e-mail: leilakarami271@yahoo.com

МОДЕЛЬ ВЫЖИВАЕМОСТИ ОПУХОЛЕВЫХ КЛЕТОК ПОСЛЕ ФОТОДИНАМИЧЕСКОЙ ТЕРАПИИ

L. Karami-Gadallo, M. Pouladian
Исламский Университет Азад, Тегеран, Иран

Резюме

При проведении фотодинамической терапии (ФДТ) индекс выживаемости (жизнеспособность) клеток в зависимости от концентрации $^1O_2$ или плотности мощности облучения на графике представляет собой кривую. В этой статье была предложена математическая модель с возможностью построения зеркально-сигмовидной кривой, которая, по мнению авторов, может быть использована для любых экспериментальных данных, касающихся жизнеспособности клеток или вероятности выживания, путем настройки трех параметров. Это было подтверждено демонстрацией совпадения кривой с данными, полученными в эксперименте *in vitro* для ФДТ с 5-аминолевулиновой кислотой клеток рака легкого.

Была предпринята попытка определить взаимосвязь между параметрами биологической модели и формой участков кривой. При низких дозах наблюдали на кривой участок плато (нечувствительная часть), при средних дозах – участок крутого подъема (высокочувствительная часть) и при высоких дозах – стационарное состояние (низкочувствительная часть). Авторы считают, что предложенная ими модель может быть применена к описанию любых данных, представляющих собой показатель выживаемости клеток, в зависимости от дозы воздействия при любом методе лечения рака (например, при лучевой терапии). Хотя это утверждение оказалось верным для ФДТ, представляется перспективной оценка пригодности предложенной модели для других данных.

Ключевые слова: кривые выживаемости клеток, математическое моделирование, фотодинамическая терапия.

Для цитирования: Karami–Gadallo L., Pouladian M. Cancer cell survival model after photodynamic therapy // Biomedical Photonics. – 2022. – Т. 11, № 2. – С. 4–11. doi: 10.24931/2413–9432–2022–11–2–4–11.

Контакты: L. Karami–Gadallo, e-mail: leilakarami271@yahoo.com

Introduction

In order to treat cancer in human, there are different techniques depending on some factors such as type and stage of cancer, specifications of 3D-contour of cancerous tissues (planned tumor volume: PTV), surrounded healthy organs (especially organs at risk: OAR), and cancer distribution from skin toward depth in the diseased organs.

In addition to traditional methods for cancer therapy such as chemotherapy, other techniques might apply photons (from low-frequency electromagnetic waves till x- and gamma-rays), accelerated massy particles (e.g. electrons, neutrons, protons and atoms) and/or mechanical waves (e.g. ultrasound beam). Such rays or beams should transfer energy into the tissues with so characteristics (i.e. spatial/temporal distribution of its intensity) that maximally kill the cancerous cells (through necrosis or apoptosis, mostly) whilst minimally harm surrounding healthy cells. In order to optimize the absorbed energies, a proper treatment plan is required. Different type/energy of any beam/ray has different interactions with the surface to inner tissues leading to different absorbed doses within them. For example, the electron beam is proper for skin and superficial cancers because of its low penetration depth (below a few cm). Although, such beams lead to apoptosis of the cells, unfortunately, generation and applying of them are relatively expensive, complicated and time consuming in addition to their ionization problems for healthy cells.

In contrast, some relatively low cost and accessible techniques are just applying non-ionization waves such as the laser or ultrasound (in the form of high intensity focused) to provide hyperthermia and necrosis in cancerous cells.

Recently, a lot of low power techniques provide some 'killer agents' between cancerous cells using a substance which would be toxic after radiation e.g. photodynamic therapy (PDT).

PDT is a promising treatment modality for cancer therapy using photosensitizer (PS), oxygen and light to destroy malignancy. Photochemical reactions between PS, light and oxygen in the cells leads to production of a cytotoxic agent known as singlet oxygen which could kill the cell. In contrast to chemotherapy and conventional radiotherapy, PDT is known as a minimally invasive technique with selectivity in cancer treatment without any complicated side effects [1-8].

The effectiveness of PDT depends on a large number of parameters including the type and dose of PS, the presenting oxygen level within the cells, the specifications of applied light (including its wavelength and irradiance and also the start/end instants of irradiation after PS incubation) and the optical properties of the tissue at the applied wavelength as well as the type and spreading out of the cancer [9]. In the cases of deep cancers (e.g. head and neck or liver cancer), PDT is performed through optical fibers to reach the light photons to cancerous region [10].

In order to determine the optimized parameters to obtain the most effectiveness of PDT, a variety of experimental and theoretical methods have been suggested by a number of researchers.

In addition to introducing the reliable techniques for PDT dosimetry, our objective in this work was to show the role of the PDT dose in the cell survival through modeling their relation. Some treatment factors (e.g. type and characteristics of drug and light), biological conditions (e.g. cancer type and its distribution) and instrumentation specifications could have main roles in selecting dosimetry method [11]. Some investigators have compared two reported PDT dosimetry techniques through measurement of the $^1O_2$ luminescence or the PS photobleaching fluorescence by which the $^1O_2$ production or the PS consumption respectively could also be tracked during treatment [12]. Some researchers have proposed a microscopic model using the six differential equations (SDE) representing the complex reactions between PS, O_2 molecules, and the emitted photons for producing $^1O_2$ which could react with nucleus receptors leading to apoptosis and cell death [13-14]. Some models quantitating PDT cytotoxicity through showing the relation between survival ratio and different types of killer agents has been introduced by some researchers [15-16]. In one survival model, in addition to the main killer agent [$^1O_2$], the unoxidized receptors concentration (denoted by [R]) was also accounted as the model's inputs [17]. In other words, they added another differential equation showing survival ratio to SDE. Unfortunately, moreover the dependency between these two inputs, [R] could not be obtained practically by measurement. It should be extracted from solving SDE with the inputs of PS concentration, photon density and some variable's initial conditions.

The PDT appears to stimulate several different signaling pathways, some of which lead to cell death, via caspase-dependent and -independent apoptosis whilst some other might cause cell survive depending on biological (e.g. cell type and cell's oxygen magnitude or hypoxia occurrence) and treatment (e.g. structure and concentration of PS, light fluence, and spatial/temporal conditions of PS distribution during irradiation) factors. Additionally, some other factors such as increased repair of induced damage to membrane, to proteins and occasionally to DNA [18], as well as cell cycle phase [19] might also cause resistant to PDT.

Based on these two different cell responses, two pathways with two different resistances against the killer agent could be imagined. Therefore, we would try to make such two-path model for estimation of cell

response with only one practical input representing a reliable killer agent (which could be [$^1O_2$], fluence or irradiation time duration).

Materials and methods

Usually, increasing PDT dose (even till infinite dose) cannot reach the cell living index (e.g. survival ratio or viability) to zero or in other words mostly there is 'non-zero steady state'. It happens because of two possible classes of reasons: measurement error of index and survivor cells.

First class of reason includes common mode factors affecting the index measurement such as background noise and recording (instrumentation) errors. Second class of reasons might correspond to hypoxia occurrence (leading to stopping $^1O_2$ generation); lack of enough PS; the cells far from access of diffused PS and/or photons; and other factors making the killing process unsuccessful (e.g. cell repair mechanisms).

Therefore, it's possible to make all of the cells to be killed under treatment by increasing PDT-dose, especially by applying simultaneously another treatment technique too (e.g. hyperthermia or photon therapy). At first, the survival index with non-zero steady state is analyzed to be modeled.

Model of nonzero steady-state survival index

Since the resistances of the cells against death determine the living index, we could divide the targets (including the cells) under applying killer agent (i.e. PDT dose) in two groups:

1. dose-independent group with constant resistance against the dose variations as shown in Fig. 1 in the form of horizontal line at resistance 40 au (arbitrary unit);

2. sensitive dose-dependent group from infinite resistance at zero dose with an ascending manner toward a residual resistance (e.g. at 20 au in Fig. 1) at infinite dose.

By paying some attentions to the data presenting the relation of index (viability or survival ratio) versus [$^1O_2$] (as PDT-dose or *d*) which obtained *in vitro* studies by a lot of researchers [17,20], it could be seen as a «hyperbolical» curve (i.e. 1/*d*) fitted between logarithm of index versus *d*. Hence, for 'sensitive cells' the relation of resistance R_s could be considered as the form of below:

$$R_s = R_\infty . e^{1/(s.d)} \quad (1)$$

In which the parameter of R_∞ is the resistance of sensitive cells at infinite *d* and *s* shows the sensitivity (in Fig. 1, *s* is 0.25 for more and 0.07 for less sensitive curves; R_∞ is 20 for both).

Two resistances of non-sensitive R_{ns} (i.e. constant R_0) and sensitive R_s (i.e. Eq. 1) act in parallel to make the total resistance of all cells as $(R_s*R_{ns})/(R_s+R_{ns})$ which simplified in the form of

$R_0/[1+(R_0/R_\infty)*\exp(-1/s*d)]$ appeared as a mirrored (right-to-left) "S"-shaped (i.e. mirrored sigmoidal).

Finally, we could present our model in the following equation to quantitate the PDT response "with nonzero steady state" (i.e. nonzero *v* at infinite *d*) as the variable v versus *d* as:

$$v(d) = \frac{v_0}{1 + m\ .e^{-1/s.d}} \quad (2)$$

where *v(d)* can be interpreted as either the cell viability, the survival index, the numbers of cells, or the probability of cell survival with setting relevant (positive) value of parameters v_0 (i.e. 100 or 1), *m*, and *s* for each one. In Fig. 2, the effect of *m* variation on the steady state (up) and *s* variation on the slope or sensitivity (down) could be seen for mirrored-sigmoid curve of Eq.2.

The parameters Concepts of the Model

In Eq. 2, the parameter v_0 means the magnitude of *v* at *d* equals to 0 (usually v_0 is 100 or 1), whilst at 'steady state' $d=\infty$ it is $v_\infty = v_0/(1+m)$. Hence, the parameter *m* could be calculated based on the initial condition v_0 and the final condition v_∞ (if presented) as follows:

$$m = (v_0 - v_\infty)/v_\infty \quad (3)$$

The parameter *s* shows the slope of descending part of mirrored sigmoid curve and relates to sensitivity.

It could be obtained by setting *d* at value 1/*s* (in Eq.2) at which *v* reaches to 1/(1+*m*/*e*) of its initial (v_0) as follows:

$$V\left(at\ d = s^{-1}\right) = \frac{V_0}{1 + me^{-1}} \quad (4)$$

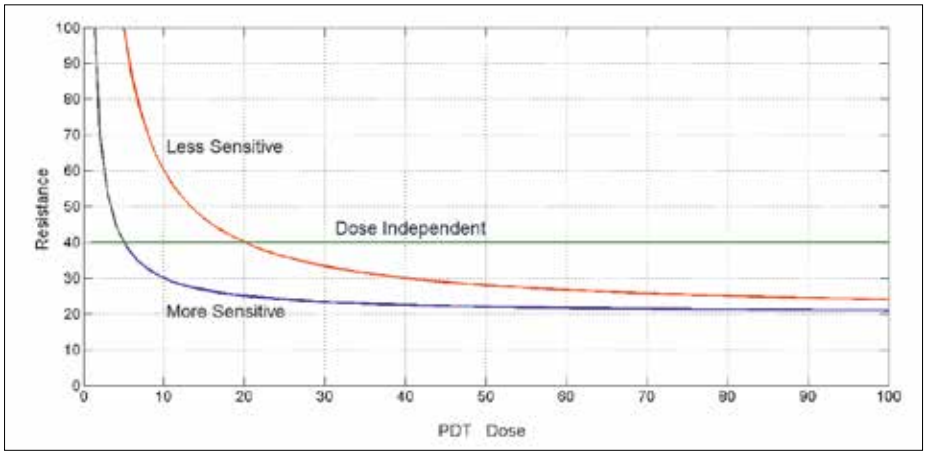

Рис. 1. Два типа устойчивости клеток при изменении параметров ФДТ: дозозависимая (два типичных случая с высокой и низкой чувствительностью) и постоянная устойчивость (нечувствительная). Оси имеют произвольные единицы измерения (усл.ед.).

Fig. 1. Two types resistances of the cells against PDT-Dose variations: dose-dependent (two typical cases with high and low sensitivity) and constant resistance (non-sensitive). The axes have arbitrary units (au).

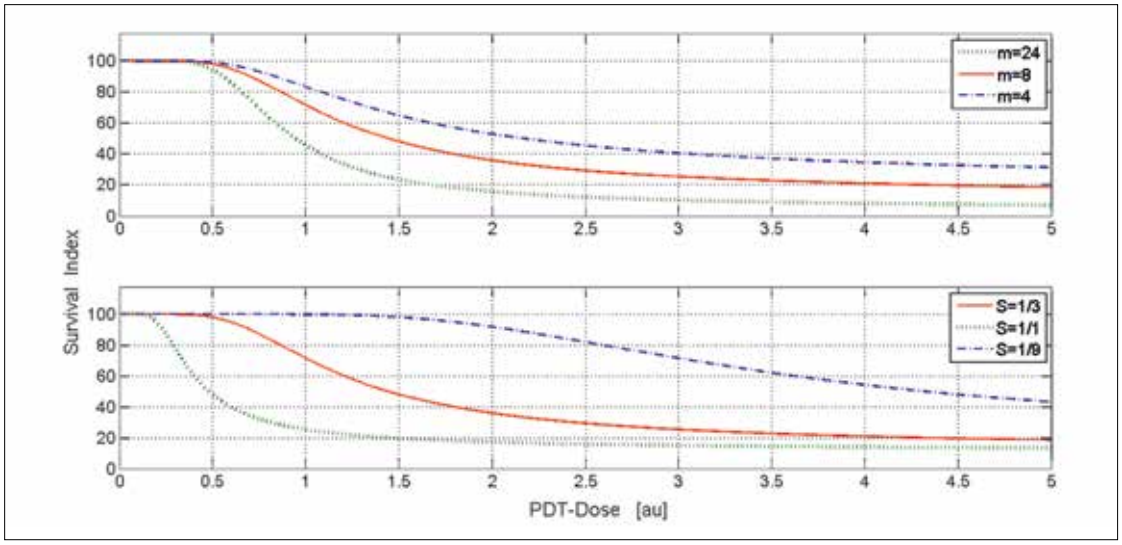

Рис. 2. Образцы зеркально-сигмовидной формы (дозы в усл.ед.) для V_0=100 и измененных двух параметров: (вверху) различные m для s=1/3; (внизу) различные s для m=8.

Fig. 2. Samples of mirrored sigmoid-shaped (with arbitrary units of the dose) for V_0=100 and altered two parameters: (Up) different m for s=1/3; (Down) different s for m=8.

One of the important points of such curves is the critical point (CP) d_c at where the curve appears linear (around d_c) with the most descending slope; and the second derivative of *v* becomes zero (i.e. $\frac{\partial^2 V}{\partial D^2}=0$ at $d=d_c$).

Therefore it could be found a relation between *Dc, m,* and *S* as follows:

$$s=\frac{1-me^{-1/(s.d_c)}}{2d_c(1+me^{-1/(s.d_c)}} \quad (5)$$

It could be shown that according to Eq.5, one could write down:

$$if\ m \ll e^2\ then\ s=1/(2d_c)$$
$$if\ m>1 then\ s<(d_c.log\ m)^{-1} \quad (6)$$

Model of Zero Steady-State Survival Index

If any cell killing-factor was added to a treatment process (e.g. adding a second therapy technique), residual sensitive cells initiated to decrease their resistance against death (i.e. decreasing R_∞) so that Rs trends to zero at high doses (i.e. steady state). Hence, Eq. 1 could be enhanced by multiplying the parameter R_∞ to an exponent term (i.e., $e^{s_2 d}$) in order to increase decaying the steady state. After affecting non-sensitive parallel resistance and some simplifications, survival index became as:

$$v(d)=\frac{v_0}{1+me^{S_2 d-1/(S_1 d)}} \quad (7)$$

that could be applied with related initial condition v_0 (*v* at zero *d*) and three parameters *m*, s_1 and s_2. By setting s_2 to zero the Eq. 7 converts to Eq. 2.

Data Acquisition

In order to validate the final model, type-II PDT data extracted from other (in vitro) work [20] was applied. The drug of 5-AminoLevulinic Acid (ALA; from 'Sigma Chemical Co') was dissolved in distilled water to obtain the stock solution (1mg/ml). After applying ALA-PDT for some 15-samples groups and providing a control group, the cell viabilities were obtained for different irradiated times for model validation.

Cell Culture

The human lung carcinoma cell (A-549) was supplied by Iranian Biological Resource Center and cultured in DMEM: Ham'SF12 + 2Mml-Glutamine+ 10% FBS in a 5% CO2 incubator at 37^{0C}. A549 cell lines were seeded into 96-well plates at concentration of 1×10^4 cells per well and were incubated for 24 hours for proper attachment to substratum. After 70–75% cell confluence, the media of wells was removed then phosphate buffered saline and 10µl 5-ALA per well added to them and incubated for 3 h.

ALA-PDT

Except the control (no ALA; no light) and ALA groups, others were irradiated with LED light (632 nm at a fixed flounce rate 35mw/cm^2) for different time durations (till 300 seconds). We repeated the test for another ALA administration too in order to obtaining 5 and 10 µl 5-ALA per well.

MTT Assay

At 24 h after the treatment, cell viabilities were obtained through MTT evaluation method using an optical densitometry technique at 570 nm measuring the activity of mitochondria and cellular dehydrogenase enzymes. The data were analyzed by one-way ANOVA statistical method in SPSS software.

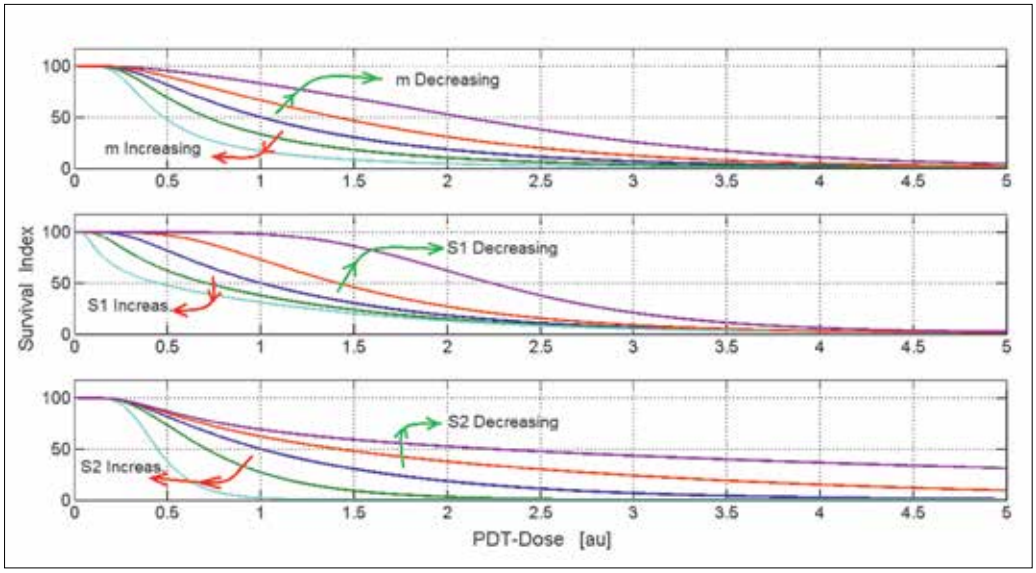

Рис. 3. Отклонения формы модели сигмоидальной кривой при значениях 1/5, 1/2, 2 и 5 для параметров m (вверху), s_1 (посередине), s_2 (внизу) относительно центральной кривая в качестве контроля с m=1, s_1=1 и s_2=1.
Fig. 3. Shape deviations of the sigmoidal-curve model for the values of 1/5, 1/2, 2, and 5 for the parameters: m (top), s_1 (middle), and s_2 (bottom) relative to central curve as the control with m=1, s_1=1, and s_2=1.

Results

We proposed a model (as shown in Eq. 7) to obtain the cell survival index (that could be cell viability, survival probability, or any index representing cell living conditions) as a function of PDT-dose (that could be illuminating time, fluence, $[^1O_2]$ or any variable representing the killer agent dose).

When experimental findings show a number of points in dose-v plane, one could extract approximately some specifications (such as the location of CP and its slope, shoulder/plateau width, vanishing speed, and the steady state magnitude) to find the model's parameters roughly.

Moreover, one could easily fit the best sigmoid-curve with the data by different mathematical techniques (found in the curve fitting toolkit of MatLab software) to obtain the optimized parameters (with minimum root mean squared error-RMSE).

In order to understand the effects of the parameters alterations on the shape of model, different magnitudes of *m*, s_1 and s_2 were applied (v_0=100) and the results compared with a control curve appeared in the central of curves in Fig. 3.

As seen in Fig. 3, the parameters could control curve features as follows:

top: *m* could control CP's slope and the ascending window width, whilst maintain approximately CP's location;

middle: s_1 could control CP's location, whilst maintain approximately its slope, hence control the plateau width,;

bottom: s_2 could control CP's slope, whilst maintain approximately its location and also the ascending window width, hence control the steady state magnitude.

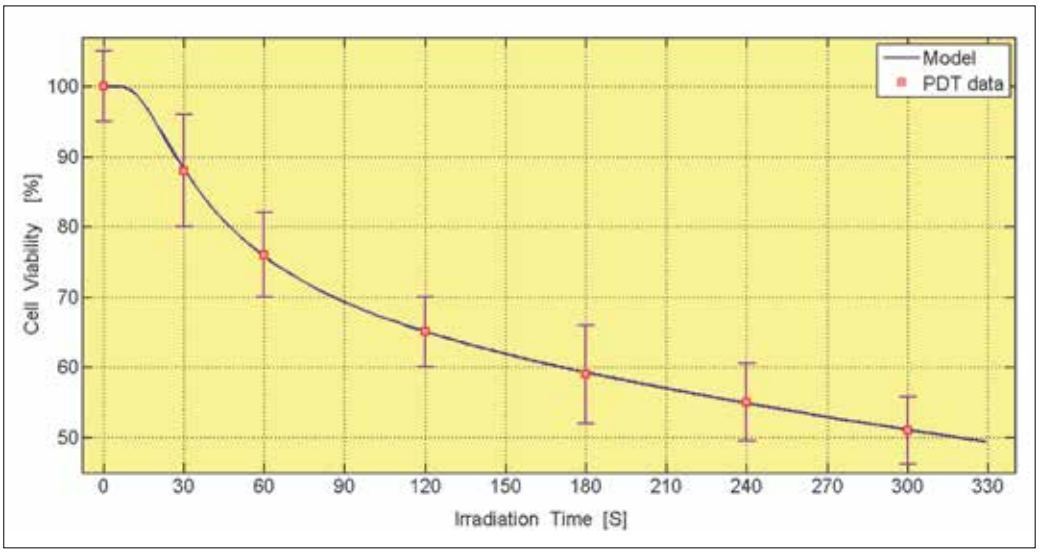

Рис. 4. Данные АЛК-ФДТ и выходные данные модели (с m = 0,6444, s_1 = 0,02052, s_2 = 0,001863)
Fig. 4. The ALA-PDT data and the model output (with m=0.6444, s_1=0.02052, s_2=0.001863)

As shown in Fig. 4, the model was validated using the obtained ALA-PDT data showing an excellent fitting relative to other models (such as single/multi target/hit inactivation, two components and linear quadratic models).

Furthermore, based on our findings, ALA did not produce considerable dark toxicity at any concentration or incubation time as verified by the MTT assay. It was found that increasing the irradiation time make the cell survival to be decreased. These findings are consistent with different ALA doses used in similar studies with other cell lines [1,3,16]. The cell death of 90% was seen (for 10 µl ALA per well) for the irradiation time of about 21 min (i.e. 24 min by the model) whilst at about 300 s (i.e. 320 s by the model) the lethal dose 50% (known as LD_{50}) observed.

By repeating the test for half ALA concentration (i.e. 5 µl per well; not shown in Fig. 4), the findings didn't vary significantly for low doses whilst a little difference for high doses (e.g. LD_{50} appeared at about 7 min) was seen.

Discussion

The PDT is a promising modality and clinically approved for treatment of certain tumors and several types of neoplasms including cutaneous lesions, non-small cell lung carcinomas, head/neck and esophageal cancers [1-8,10,21]. In PDT researches, presenting multifactorial and complex photochemical processes (e.g. multi molecular interaction, spatial/temporal variation of the concentration before and during the irradiation time) could cause challenging problems in the analysis and dosimetry of PDT and hence limit the related studies variety.

This study was designed firstly to determine the effect of varying the ALA-mediated PDT dose (i.e. different flounce; or irradiation time here) on the survival of non-small cells of lung carcinoma (in vitro) and secondly to model mathematically their relation.

It could be noticed that the relation curve between the cell survival and the killer agent in all of the cancer treatment methods (even including radiotherapy) has a mirrored sigmoidal form such as radiobiological models (e.g. m-hits n-targets or linear quadratic models) [22].

However, it could be imagined that for any survival curve there are approximately three ideal main regions: the plateau (negligible effect; a bit cell death at low doses), the descending slope (the most sensitivity; the most killing rate at the critical dose) and the steady state segment as shown in Fig. 5.

In Eq.7, the survival index *v* could be approximately (assuming error under 10%) equivalent to $1/[1+m*\exp(-1/(s_1*d)]$ for low doses (i.e., $d < 1/(10*s_2)$, and $1/[1+m*\exp(s_2*d)]$ for high doses ($d > 10/s_1$). Hence, these three geometric features (as shown in Fig. 5) could be determined through three parameters of the model (as could be noticed in Fig. 2). Nonetheless, the features could be visualized to have some proportional relations with the most affectivity parameters as follows:

$$s_1 \downarrow \Rightarrow plateau\ width \uparrow$$

$$m \uparrow or\ s_2 \uparrow \Rightarrow slope \uparrow \quad (\text{if } d > 1/m \text{ then } s_2 \text{ is more affective else, } m \text{ is})$$

$$m \downarrow or\ s_2 \downarrow \Rightarrow tail\ height \uparrow \quad (\text{if } d > 1/m \text{ then } s_2 \text{ is more affective else, } m \text{ is}) \quad (7)$$

Hence, from biological viewpoint, the sensitivity parameters (i.e., s_1 and s_2) and the sensitivity magnifier parameter (i.e., *m*) could be mostly interpreted as follows:

The 'cell killing dose threshold' could be controlled mostly by s_1; whilst the 'cell killing velocity' by s_2 and the 'steady-state survived cells' by *m*.

Also, from biochemical viewpoint, it could be said: the more affective and proper of PS, the more s_2 value; the more diehard and resistant of the cells against killer agent, the less s_1; the more concentration of PS and oxygen, the more *m* value.

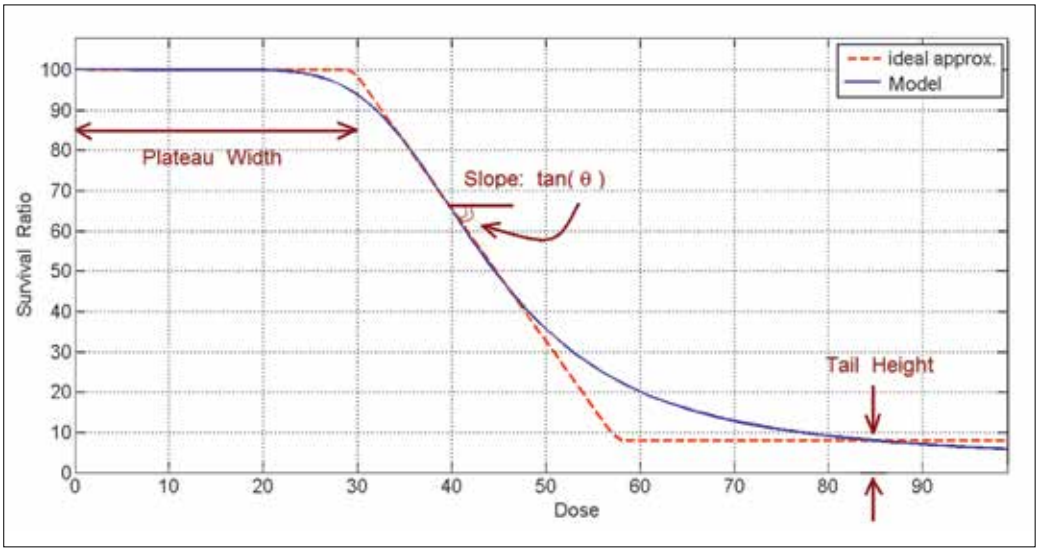

Рис. 5. Пример модели (с параметрами: m=491, s_1=0,00385, s_2=0)
Fig. 5. A sample of the model (with parameters: m=491, s_1=0.00385, s_2=0).

However, accurate biological interpretation of our model's parameters is still unknown as well as other model's ones.

From the mathematical view (i.e. MSER), our model could fit better than other models (e.g., target-theory based models [23]) on the obtained PDT-data (MSER findings were not presented here).

If a treatment technique could not kill all of the cancerous cells (i.e. constant steady sate), the model of Eq.2 (or Eq.7 with s_2=0) might be applied with two parameters (as follows: *m* depending on the requirements of the technique (e.g., PS and oxygen concentrations) and target conditions (e.g., the population rate of non-sensitive cells); and *s* depending on the effectiveness of the killer agent (i.e. the sensitivity). According to Fig. 5, it could be said that the more *m*, the less tail height whilst the more s, the more slope and the less plateau width. If a second treatment technique is also applied simultaneously, one might use its sensitivity as s_2 in the model Eq.7.

The presented model could show a plateau or shoulder on the cell survival curve whose size could be varied by the model parameters (i.e. mostly s_1) based on the technique performance in low doses. Moreover, in contrast to other models (including two compartment and/or linear quadratic ones), the curve maintains its sigmoid shape even in logarithmic scales (not shown in figures here) which is consistent with experiments.

In order to modeling of the viability, survival probability, and the population of the cells, v_0 in Eq.7 should be set respectively to 100, 1, and the cells initial number.

By using a radioisotope in 'for example gamma camera', a variable presenting cellular metabolism could be obtained from an image of cancerous region. On the other hand, the absorbed dose of related killer agent (e.g. x-ray or electron-beam) could also be measured by relevant dosimetry technique. Hence, obtaining the metabolism level versus different treatment doses could provide some data in the form of various points in the dose-metabolism plane.

It seems model of Eq.7 could fit a proper curve on such data better than other models [22] could. «Encompassing the most fitness on real cellular response to any killer agent» for our model is the statement that we are working on its validity.

Conclusion

A mathematical model (with three parameters m, S_1, and S_2) was proposed which seems to be fitted better than other models on the cell survival data versus the killer agent dose. Here, it was tested for the cell viability data versus different irradiation time durations in ALA-PDT (on the lung cancerous cells in vitro) resulting excellent fitting. The mirrored (right-to-left) sigmoid curve generated from this model had a shoulder as usually needed for mammalian survival curve; moreover, this curve kept its nonlinear-shape in semi-logarithmic scale. By tuning three parameters of the model, it could make any required form in the survival curve for both regions of low doses (slow variations) and high doses (steady-state) as well as the descending part (which is linear about the steepest point). However, it is needed to test this model by the survival data of any cancer-therapy technique applied by other researchers. It is also essential to consider the correlations between the model's parameters and treatment factors in order to obtain the best biological interpretations for the parameters.

Acknowledgement

The authors would like to thank Sama Pouladian for her help in providing figures. This research did not receive any specific grant from funding agencies in the public-commercial, or non-for-profit sectors.

REFERENCES

1. Girotti A. Photodynamic Therapy of Neoplastic Disease, *CRC Press*, Boca Raton, FL, USA: 1990.
2. Filonenko E.V. Clinical implementation and scientific development of photodynamic therapy in Russia in 2010-2020, *Biomedical Photonics*, 2021, vol. 10, no. 4, pp. 4–22. doi: 10.24931/2413–9432–2021–9-4-4-22
3. Sokolov V.V., Filonenko E.V., Telegina L.V. et al. Combination of fluorescence imaging and local spectrophotometry in fluorescence diagnostics of early cancer of larynx and bronchi, *Quantum Electronics*, 2002, vol. 32, no. 11, pp. 963–969. doi: 10.1070/QE2002v032n11ABEH002329
4. Agostinis P. et al. Photodynamic therapy of cancer: an update, *CA Cancer J. Clin*., 2011, vol. 61 (4), pp. 250–281.
5. Filonenko E.V., Kaprin A.D., Raszhivina A.A., Urlova A.N., Nechipai A.M. Fluorescence diagnostics of colon

ЛИТЕРАТУРА

1. Girotti A. Photodynamic Therapy of Neoplastic Disease // CRC Press; Boca Raton, FL, USA: 1990.
2. Filonenko E.V. Clinical implementation and scientific development of photodynamic therapy in Russia in 2010-2020 // Biomedical Photonics. – 2021. – Т. 10, № 4. – С. 4–22. doi: 10.24931/2413-9432-2021-9-4-4-22
3. Sokolov V.V., Filonenko E.V., Telegina L.V., Boulgakova N.N., Smirnov V.V. Combination of fluorescence imaging and local spectrophotometry in fluorescence diagnostics of early cancer of larynx and bronchi // Quantum Electronics. – 2002. – Vol. 32(11). – P. 963–969. doi: 10.1070/QE2002v032n11ABEH002329
4. Agostinis P. et al. Photodynamic therapy of cancer: an update // CA Cancer J. Clin. – 2004. Vol. 61 (4) – P. 250–281.
5. Filonenko, E.V., Kaprin, A.D., Raszhivina, A.A., Urlova, A.N., Nechipai, A.M. Fluorescence diagnostics of colon malignant and premalignant

malignant and premalignant lesions using 5-aminolevulinic acid, *International Journal of Photoenergy*, 2014, no. 378673. doi: 10.1155/2014/378673
6. Filonenko E.V., Ivanova-Radkevich V.I. Photodynamic therapy in the treatment of patients with mycosis fungoides, *Biomedical Photonics*, 2022, vol. 11, no. 1, pp. 27–36. doi: 10.24931/2413–9432–2022–11-1-27-36.
7. Henderson B.W., Dougherty T.J. How does photodynamic therapy work? *Photochem. Photobiol.*, 1992, vol. 55, pp. 145–157.
8. Filonenko E.V. The history of development of fluorescence diagnosis and photodynamic therapy and their capabilities in oncology, *Russian Journal of General Chemistry*, 2015, vol. 85(1), pp. 211–216. doi: 10.1134/S1070363215010399
9. Helander L., Krokan H.E., Johnsson A., Gederaas O.A., Plaetzer K. Red versus blue light illumination in hexyl 5-aminolevulinate photodynamic therapy: the influence of light color and irradiance on the treatment outcome in vitro, *Journal of Biomedical Optics*, 2014, vol. 19(8), pp. 088002.
10. Jerjes W., Upile T., Betz C.S., El Maaytah M., Abbas S., Wright A. et al. The application of photodynamic therapy in the head and neck, *Dent Update*, 2017, vol. 34, pp. 478-486.
11. Zheng Huang et al. Photodynamic therapy for treatment of solid tumors – potential and technical challenges, *Technol Cancer Res Treat*, 2008, vol. 7(4), pp. 309–320.
12. Jarvi M.T., Patterson M.S., Wilson B.C. Insights into Photodynamic Therapy Dosimetry: Simultaneous Singlet Oxygen Luminescence and Photosensitizer Photobleaching Measurements, *Biophysical Journal Volume*, 2012, vol. 102, pp. 661–671.
13. Foster, T.H., Murant R.S., Bryant R.G., Knox R.S., Gibson S. L. and Hilf R. Oxygen consumption and diffusion effects in photodynamic therapy, *Radiat. Res.*, 1991, vol. 126, pp. 296–303.
14. Valentine R.M., Ibbotson S.H., Wood K., Brown C.T. Modelling fluorescence in clinical photodynamic therapy, *Photochem Photobiol Sci*, 2013, vol. 12(1), pp. 203–13 [PubMed: 23128146]
15. Pelicano H., Carney D. and Huang P. ROS stress in cancer cells and therapeutic implications, *Drug Resist. Updat.*, 2014, vol. 7, pp. 97–110.
16. Belousova I. M., Mironova N.G. and Yur'ev M.S. A mathematical model of the photodynamic fullerene-oxygen action on biological tissues, *Opt. Spectrosc*, 2015, vol. 98, pp. 349–356.
17. Ioannis Gkigkitzis, Yuanming Feng, Chunmei Yang, Jun Q. Lu and Xin-Hua Hu. Modeling of Oxygen Transport and Cell Killing in Type-II Photodynamic Therapy, *Photochemistry and Photobiology*, 2012, vol. 88, pp. 969–977.
18. Casasa A., Di Venosa G., Hasan T. and Batllea A. Mechanisms of Resistance to Photodynamic Therapy, *Curr Med Chem*, 2011, vol. 18(16), pp. 2486–2515.
19. Wyld L., Smith O., Lawry J., Reed M.W. and Brown N.J. Cell cycle phase influences tumour cell sensitivity to aminolaevulinic acid-induced photodynamic therapy in vitro, *Br J Cancer*, 1998, vol. 78(1), pp. 50–55.
20. Karami Gadallo L., Ghoranneviss M., Ataie-Fashtami L., Pouladian M., Sardari D., Enhancement of Cancerous Cells Treatment by Applying Cold Atmosphere Plasma and Photo Dynamic Therapy Simultaneously, *Clinical Plasma Medicine*, 2017 http://dx.doi.org/10.1016/j.cpme.2017.08.002
21. Chen X., Zhao P., Chen F., Li L., and Luo R. Effect and mechanism of 5-aminolevulinic acid-mediated photodynamic therapy in esophageal cancer, *Lasers Med Sci*, 2011, vol. 26, pp. 69-78.
22. Bodgi L. et al. Mathematical models of radiation action on living cells: From the target theory to the modern approaches. A historical and critical review, *Journal of Theoretical Biology*, 2011, vol. 394, pp. 93 –101.
23. Nomiya T. Discussions on target theory: past and present, *J Radiat Res*, 2013, vol. 54(6), pp. 1161–1163.

lesions using 5-aminolevulinic acid // International Journal of Photoenergy. – 2014. – № 378673 Doi: 10.1155/2014/378673
6. Filonenko E.V., Ivanova-Radkevich V.I. Photodynamic therapy in the treatment of patients with mycosis fungoides // Biomedical Photonics. – 2022. – T. 11, № 1. – C. 27–36. doi: 10.24931/2413–9432–2022–11-1-27-36.
7. Henderson B.W., Dougherty T.J. How does photodynamic therapy work? // Photochem. Photobiol. – 1992. – Vol. 55. – P. 145–157.
8. Filonenko E.V. The history of development of fluorescence diagnosis and photodynamic therapy and their capabilities in oncology // Russian Journal of General Chemistry. – 2015. – Vol. 85(1). – P. 211–216. doi: 10.1134/S1070363215010399
9. Helander L., Krokan H.E., Johnsson A., Gederaas O.A., Plaetzer K. Red versus blue light illumination in hexyl 5-aminolevulinate photodynamic therapy: the influence of light color and irradiance on the treatment outcome in vitro // Journal of Biomedical Optics. – 2014. – Vol. 19(8). – P. 088002.
10. Jerjes W., Upile T., Betz C.S., El Maaytah M., Abbas S., Wright A. et al. The application of photodynamic therapy in the head and neck // Dent Update. 2017. – Vol. 34. – P. 478-486.
11. Zheng Huang et al. Photodynamic therapy for treatment of solid tumors – potential and technical challenges // Technol Cancer Res Treat. – 2008. – Vol. 7(4). – P. 309–320.
12. Jarvi M.T., Patterson M.S., Wilson B.C. Insights into Photodynamic Therapy Dosimetry: Simultaneous Singlet Oxygen Luminescence and Photosensitizer Photobleaching Measurements // Biophysical Journal Volume. – 2012. – Vol. 102. – P. 661–671.
13. Foster, T.H., Murant R.S., Bryant R.G., Knox R.S., Gibson S. L. and Hilf R. Oxygen consumption and diffusion effects in photodynamic therapy // Radiat. Res. – 1991. – Vol. 126. – P. 296–303.
14. Valentine R.M., Ibbotson S.H., Wood K., Brown C.T. Modelling fluorescence in clinical photodynamic therapy // Photochem Photobiol Sci. – 2013. – Vol. 12(1). – P. 203–13 [PubMed: 23128146]
15. Pelicano H., Carney D. and Huang P. ROS stress in cancer cells and therapeutic implications // Drug Resist. Updat. – 2014. – Vol. 7. – P. 97–110.
16. Belousova I. M., Mironova N.G. and Yur'ev M.S. A mathematical model of the photodynamic fullerene-oxygen action on biological tissues // Opt. Spectrosc. – 2015. –Vol. 98. – P. 349–356.
17. Ioannis Gkigkitzis, Yuanming Feng, Chunmei Yang, Jun Q. Lu and Xin-Hua Hu. Modeling of Oxygen Transport and Cell Killing in Type-II Photodynamic Therapy // Photochemistry and Photobiology. – 2012. – Vol. 88. – P. 969–977.
18. Casasa A., Di Venosa G., Hasan T. and Batllea A. Mechanisms of Resistance to Photodynamic Therapy // Curr Med Chem. – 2011. – Vol. 18(16). – P. 2486–2515.
19. Wyld L., Smith O., Lawry J., Reed M.W. and Brown N.J. Cell cycle phase influences tumour cell sensitivity to aminolaevulinic acid-induced photodynamic therapy in vitro // Br J Cancer. 1998. – Vol. 78(1). – P. 50–55.
20. Karami Gadallo L., Ghoranneviss M., Ataie-Fashtami L., Pouladian M., Sardari D., Enhancement of Cancerous Cells Treatment by Applying Cold Atmosphere Plasma and Photo Dynamic Therapy Simultaneously // Clinical Plasma Medicine. – 2017. http://dx.doi.org/10.1016/j.cpme.2017.08.002
21. Chen X., Zhao P., Chen F., Li L., and Luo R. Effect and mechanism of 5-aminolevulinic acid-mediated photodynamic therapy in esophageal cancer // Lasers Med Sci. – 2011. –Vol. 26. – P. 69-78.
22. Bodgi L. et al. Mathematical models of radiation action on living cells: From the target theory to the modern approaches. A historical and critical review // Journal of Theoretical Biology. – 2011. – Vol. 394. – P. 93 –101.
23. Nomiya T. Discussions on target theory: past and present // J Radiat Res. – 2013. – Vol. 54(6). – P. 1161–1163.